Iranian Journal of Science and Technology, Transactions of Mechanical Engineering (2022) 46:927–942
https://doi.org/10.1007/s40997-021-00464-y

RESEARCH PAPER

Moving Contact Problem of an Unbonded Layer in the Presence of Body Force

İsa Çömez[1]

Received: 31 May 2021 / Accepted: 15 October 2021 / Published online: 28 October 2021

Abstract
In this study, moving continuous and discontinuous contact problems of a layer were examined in the presence of body force. The unbonded layer was pressed to a rigid foundation by a rigid cylindrical punch that moved over the layer steadily. In the presence of body force, for the moving contact problem, the general stress and displacement expressions were derived using the theory of elasticity and Fourier integral transforms, without using the superposition technique. Through applying the boundary conditions of the problem, the singular integral equations in which the contact stresses and contact areas were unknown were obtained for both the continuous and discontinuous contact cases. The singular integral equations were solved numerically using the Gauss–Chebyshev integration formula. Numerical results for critical load, initial separation distance, the separation region, contact stress distributions under the punch and between the layer, and foundation were given for various dimensionless quantities.

Keywords Contact problem · Continuous contact · Discontinuous contact · Body force · Separation · Singular integral equation · Fourier transforms

1 Introduction

Since loads are transmitted through contacting components in many practical engineering applications, contact problems have gained an important role in solid mechanics. Contact stress, contact area, contact type, and deformation at the contact surfaces remarkably affect the behavior of engineering structures such as road pavements, foundations, railway ballasts, brake disks, and abradable seals in gas turbine components.

Studies related to the contact problem can be classified into four groups based on the separation types: bonded contact, receding contact, continuous contact, and discontinuous contact.

In bonded contact problems, it is assumed that contacting bodies are fully bonded to each other and the separation of them is not possible whatever the value of the load is. Recent studies related to contact problems have focused on functionally graded materials (FGMs). FGMs are a new class of composite materials whose compositions and microstructures vary continuously in any direction. Assuming the exponential variation of the shear modulus, Guler and Erdogan (2004, 2007) investigated the plane strain sliding contact problem of an FG layer bonded to a homogeneous half plane. The loading is provided by a rigid cylindrical or flat punch. Ke and Wang (2006, 2007) and Yang and Ke (2008) developed the multilayered model for the frictional and frictionless contact problems with arbitrary varying material properties. In this model, the FGM was divided into sublayers in which the shear modulus varied linearly from one surface to another. The axisymmetric contact problem of an FM layer bonded to a homogeneous half plane was studied by Liu and Wang (2008) and Liu et al. (2008) using the Hankel transform technique. In the study of Chen and Chen (2012), the layer was assumed as linearly graded. The layer is indented by a concentrated normal force or by a rigid cylindrical stamp. Choi (2009) examined the frictional contact problem of a single FG layer bonded to a rigid foundation. Çömez and Guler (2017) studied the sliding contact problem of an FG bilayer indented by a rigid cylindrical punch. Chen et al. (2017) and Chen et al. (2019) investigated the interfacial analysis of a thin film bonded to a finite-thickness graded substrate under different loading conditions.

✉ İsa Çömez
isacomez@ktu.edu.tr; isacomez@hotmail.com

[1] Civil Engineering Department, Karadeniz Technical University, 61080 Ortahisar, Trabzon, Turkey

Chen et al. (2018) examined a thin piezoelectric actuator attached to a graded half plane with an adhesive layer under electrical loading. Peng et al. (2019) investigated a frictional contact problem of an arbitrarily oriented substrate loaded by a rigid flat indenter.

In receding contact problems, contacting components are not bonded to each other, and the body forces are ignored. Thus, the separation begins when the effect of the external load vanishes. Because the body force is ignored, the separation lasts infinitely. Receding double-contact problems of two layers bonded to a rigid foundation and indented by a rigid cylindrical punch were solved by Comez et al. (2004), Yan and Li (2015), and Çömez et al. (2016). The layers were assumed as homogeneous by Comez et al. (2004), the upper layer as FG and the lower layer as homogeneous by Yan and Li (2015), and both layers as FG by Çömez et al. (2016). The plane receding contact problem between the layer and a homogeneous half plane was investigated by Kahya et al. (2007a, b) and El-Borgi et al. (2006). The layer was assumed as anisotropic (Kahya et al., 2007a, b) and FG (El-Borgi et al., 2006). The axisymmetric receding contact problem between the FG layer and a homogeneous half plane was solved by Rhimi et al. (2009) and Liu et al. (2016) using the Hankel transform technique. Adıyaman et al. (2016) investigated the receding contact problem of a homogeneous or FG layer resting on a quarter plane and loaded by a symmetrical distributed load. Adibelli et al. (2013) and Yan and Mi (2017a, 2017b) studied the bilayer resting on a half plane. Frictional receding contact problems are more complex than frictionless contact problems because the unknown contact areas increase, and there are not many studies about this issue. Çömez (2010), El-Borgi et al. (2014), El-Borgi and Çömez (2017), and Yilmaz et al. (2018) investigated the frictional receding contact problem between a FG/homogeneous layer and a homogeneous half plane/FG layer. Parel and Hills (2016) studied the frictional receding contact problem between a homogeneous layer and a half plane when the layer was loaded by a semi-infinite uniform normal surface pressure.

In the studies mentioned before, the body forces are neglected. However, in continuous and discontinuous (CDC) contact problems, body forces are taken into account, and it is assumed that contacting components are not bonded to each other. Hence, two types of contact occur depending on the value of the external load: continuous contact and discontinuous contact. When the external load is less than a certain critical value, no separation occurs between the contacting bodies, and the contact will be continuous throughout the components interface. Thus, the main problem of the continuous contact issue is to find the critical load that causes separation. If the external load exceeds the certain critical value, separation occurs between contacting components, and this type of contact is called discontinuous. In the study of Civelek and Erdogan (1975), the elastic layer lying on a rigid foundation was subjected to the concentrated vertical lifting force. Gecit and Erdogan (1978) extended this study to the axisymmetric case. The elastostatic problem of a layer resting on a half space was studied by Gecit (1980). The layer was subjected to the uniform clamping pressure as well as the concentrated vertical line load. Çakıroğlu et al. (2001) studied the CDC contact problem of two layers resting on a half plane. They examined the separation regions between the upper and lower layer and between the lower layer and half plane. Kahya et al. (2007a, b) studied the continuous contact problem of two orthotropic layers indented by a rigid flat-ended stamp. Ozsahin and Taşkıner (2013) investigated the CDC contact problem of a layer lying on a half plane. The layer was loaded via three rigid flat punches. Öner et al. (2017) and Adıyaman et al. (2017) examined the CDC contact problem of an FG layer. Çömez (2019) studied the CDC contact problem of an FG layer pressed to a rigid foundation by a rigid cylindrical punch. Polat et al. (2018) and Kaya et al. (2020) studied the CDC problem of an FG layer indented by two rigid flat punches.

Although there are many studies related to static contact problems in the literature, moving continuous and discontinuous contact problems have not been discussed yet. In this study, the effects of velocity on continuous and discontinuous contact problems are examined when the layer is indented by a rigid cylindrical punch, and stress and displacement expressions are derived without using the superposition technique.

2 General Equations for Stresses and Displacements

In this part, general expressions for the stresses and the displacements will be obtained without asserting the superposition method used by the previous researchers.

The geometries of the continuous and discontinuous contact problems of an isotropic and homogeneous layer are shown in Figs. 1 and 2, respectively. The layer with the height h is subjected to a concentrated normal force P by means of a rigid cylindrical punch with radius R. The rectangular coordinates (x_1, y_1) are fixed in the layer, and the translating coordinates (x, y) are attached to the rigid punch.

The differential equations of motion for the case of plane strain may be written as

$$\frac{\partial \sigma_x}{\partial x_1} + \frac{\partial \tau_{xy}}{\partial y_1} = \rho \frac{\partial^2 u}{\partial t^2} \tag{1}$$

$$\frac{\partial \tau_{yx}}{\partial x_1} + \frac{\partial \sigma_y}{\partial y_1} - \rho g = \rho \frac{\partial^2 v}{\partial t^2} \tag{2}$$

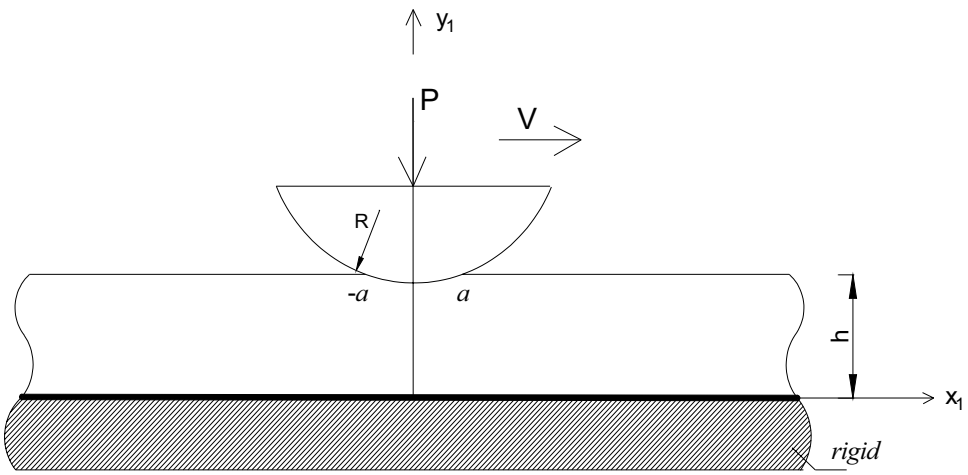

Fig. 1 Geometry of the continuous moving contact problem

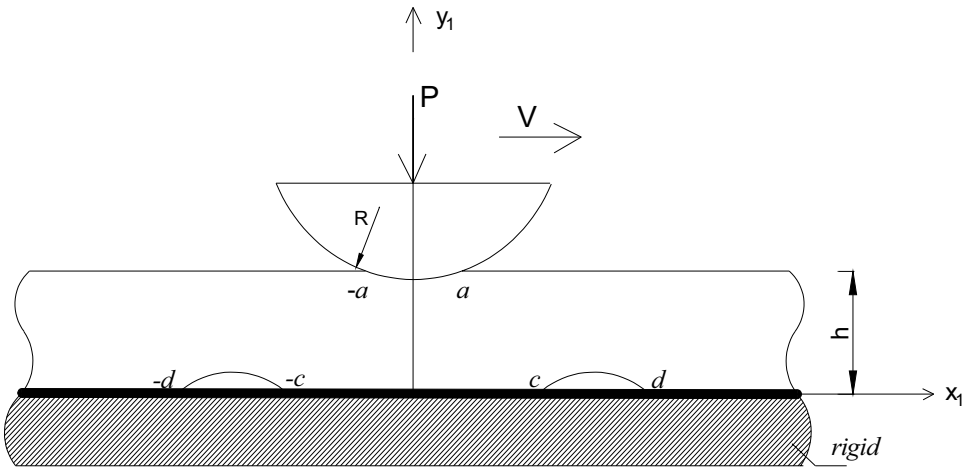

Fig. 2 Geometry of the discontinuous moving contact problem

where ρ is the mass density per unit volume of the layer and g is the gravitational acceleration.

The layer is assumed to be homogeneous, isotropic, and linearly elastic. Hence, for the plane strain contact problem, stress–displacement relation can be written as follows:

$$\sigma_x(x,y) = \frac{\mu}{\kappa-1}\left[(\kappa+1)\frac{\partial u}{\partial x_1} + (3-\kappa)\frac{\partial v}{\partial y_1}\right] \tag{3}$$

$$\sigma_y(x,y) = \frac{\mu}{\kappa-1}\left[(3-\kappa)\frac{\partial u}{\partial x_1} + (\kappa+1)\frac{\partial v}{\partial y_1}\right] \tag{4}$$

$$\tau_{xy} = \mu\left[\frac{\partial u}{\partial y_1} + \frac{\partial v}{\partial x_1}\right] \tag{5}$$

where u and v are the x_1 and y_1 components of the displacement vector, ν is the Poisson's ratio, and $\kappa = 3 - 4\nu$ for the plane strain case. μ is the shear modulus of the layer.

The dynamic contact problem can be reduced to the steady contact problem by using the following coordinate transformation:

$$x = x_1 - Vt \; y = y_1 \tag{6}$$

Substituting Eqs. (2) and (3) into the equilibrium Eqs. (1) and (2), the following partial differential equations are obtained in terms of $u(x, y)$ and $v(x, y)$:

$$(\kappa+1)\frac{\partial^2 u}{\partial x^2} + (\kappa-1)\frac{\partial^2 u}{\partial y^2} + 2\frac{\partial^2 v}{\partial x \partial y} - (\kappa-1)\frac{V^2\rho}{\mu}\frac{\partial^2 u}{\partial x^2} = 0 \tag{7}$$

$$(\kappa-1)\frac{\partial^2 v}{\partial x^2} + (\kappa+1)\frac{\partial^2 v}{\partial y^2} + 2\frac{\partial^2 u}{\partial x \partial y} - (\kappa-1)\frac{V^2\rho}{\mu} = (\kappa-1)\frac{\rho g}{\mu} \tag{8}$$

Using the Fourier integral transforms, the system of the partial differential equations can be reduced to the ordinary differential equations. Therefore, the displacement components are taken as the following transformed form:

$$u(x,\ y) = \frac{1}{2\pi}\int_{-\infty}^{\infty} \tilde{u}(\alpha,\ y)\, e^{-I\alpha x} d\alpha \tag{9}$$

$$v(x,\ y) = \frac{1}{2\pi}\int_{-\infty}^{\infty} \tilde{v}(\alpha,\ y)\, e^{-I\alpha x} d\alpha \tag{10}$$

where I denotes the imaginary unit, and $\tilde{u}(\alpha, y)$ and $\tilde{v}(\alpha, y)$ are the Fourier transforms of $u(x, y)$ and $v(x, y)$, respectively. Applying the Fourier transforms (5) to Eqs. (4) and (7) with respect to x, the following ordinary differential equation system is obtained:

$$(\kappa-1)\frac{d^2\tilde{u}}{dy^2} - 2I\alpha\frac{d\tilde{v}}{dy} - \alpha^2(\kappa+1)\tilde{u} + \alpha^2(\kappa-1)\frac{V^2\rho}{\mu}\tilde{u} = 0 \tag{11}$$

$$\begin{aligned}(\kappa+1)\frac{\partial^2\tilde{v}}{\partial y^2} - 2I\alpha\frac{\partial\tilde{u}}{\partial y} - \alpha^2(\kappa-1)\,\tilde{v} \\ + \alpha^2(\kappa-1)\frac{V^2\rho}{\mu}\tilde{v} = (\kappa-1)\frac{\rho g}{\mu}\delta(\alpha)\end{aligned} \tag{12}$$

where δ denotes the Dirac delta function. After some lengthy but straightforward mathematical operations shown in Eq. (6), the following nonhomogeneous ordinary differential equation is achieved:

$$(\kappa+1)\frac{d^4\tilde{v}}{dy^4} + L_1\frac{d^2\tilde{v}}{dy^2} + L_2\tilde{v} = -\alpha^2\frac{\rho g}{\mu}(1+\kappa+(1-\kappa)\frac{V^2\rho}{\mu})\delta(\alpha) \tag{13}$$

where

$$L_1 = 2\alpha^2\left(\kappa\left(-1+\frac{V^2\rho}{\mu}\right)-1\right) \tag{14}$$

$$L_2 = -\alpha^4\left(-1+\frac{V^2\rho}{\mu}\right)\left(\kappa+1-(\kappa-1)\frac{V^2\rho}{\mu}\right) \tag{15}$$

The solution of Eqs. (11 and 12) can be obtained as

$$\begin{aligned}\tilde{v}(\alpha,y) =& A_1 e^{n_1|\alpha|y} + A_2 e^{n_2|\alpha|y} + A_3 e^{n_3|\alpha|y} \\ &+ A_4 e^{n_4|\alpha|y} - \frac{\rho g/\mu}{\alpha^2(1-V^2\rho/\mu)}\delta(\alpha)\end{aligned} \tag{16}$$

where

$$n_1 = -n_2 = \sqrt{1-\frac{V^2\rho}{\mu}} \tag{17}$$

$$n_3 = -n_4 = \sqrt{1-(\frac{\kappa-1}{\kappa+1})\frac{V^2\rho}{\mu}} \tag{18}$$

Using Eq. (16) and (9 and 10), the tangential displacement $\tilde{u}(\alpha, y)$ can be written as follows:

$$\begin{aligned}\tilde{u}(\alpha,y) =& I\frac{|\alpha|}{\alpha}\left(-A_1 n_1 e^{n_1|\alpha|y} + A_2 n_2 e^{n_2|\alpha|y}\right. \\ &\left. + \frac{1}{n_3}A_3 e^{n_3|\alpha|y} + \frac{1}{n_4}A_4 e^{n_4|\alpha|y}\right)\end{aligned} \tag{19}$$

Substituting Eqs. (9, 10, 11) into Eq. (5), the displacement expressions for the layer are obtained as

$$\begin{aligned}u(x,y) =& \frac{1}{2\pi}\int_{-\infty}^{\infty}\left[I\frac{|\alpha|}{\alpha}\left(-A_1 n_1 e^{n_1|\alpha|y} + A_2 n_2 e^{n_2|\alpha|y}\right.\right. \\ &\left.\left. + \frac{1}{n_3}A_3 e^{n_3|\alpha|y} + \frac{1}{n_4}A_4 e^{n_4|\alpha|y}\right)\right] e^{-I\alpha x} d\alpha\end{aligned} \tag{20}$$

$$v(x,y) = \frac{1}{2\pi}\int_{-\infty}^{\infty}\left[A_1 e^{n_1|\alpha|y} + A_2 e^{n_2|\alpha|y} + A_3 e^{n_3|\alpha|y} + A_4 e^{n_4|\alpha|y} - \frac{\rho g/\mu}{\alpha^2(1-V^2\rho/\mu)}\delta(\alpha)\right] e^{-I\alpha x} d\alpha \tag{21}$$

Substituting Eqs. (20 and 21) into Eqs. (3, 4, 5), the stress components for the layer can be obtained as follows:

$$\frac{\sigma_x(x,y)}{\mu} = \frac{1}{2\pi}\int_{-\infty}^{\infty}|\alpha|\left[-2A_1 n_1 e^{n_1|\alpha|y} - 2A_2 n_2 e^{n_2|\alpha|y} + A_3\frac{1}{n_3}m_1 e^{n_3|\alpha|y} + A_4\frac{1}{n_4}m_1 e^{n_4|\alpha|y}\right] e^{-I\alpha x} d\alpha \tag{22}$$

$$\frac{\sigma_y(x,y)}{\mu} = \frac{1}{2\pi}\int_{-\infty}^{\infty}|\alpha|\left[2A_1 n_1 e^{n_1|\alpha|y} - 2A_2 n_2 e^{n_2|\alpha|y} - A_3\frac{1}{n_3}m_2 e^{n_3|\alpha|y} + A_4\frac{1}{n_4}m_2 e^{n_4|\alpha|y}\right] e^{-I\alpha x} d\alpha \tag{23}$$

$$\frac{\tau_{xy}(x,y)}{\mu}=\frac{1}{2\pi}\int_{-\infty}^{\infty}\alpha I\left[A_1m_2e^{n_1|\alpha|y}+A_2m_2e^{n_2|\alpha|y}-2A_3e^{n_3|\alpha|y}+A_4e^{n_4|\alpha|y}+\frac{\rho g/\mu}{\alpha^2(1-V^2\rho/\mu)}\delta(\alpha)\right]e^{-I\alpha x}d\alpha \tag{24}$$

where

$$m_1=\left(\frac{\kappa-3}{\kappa+1}\right)\frac{V^2\rho}{\mu}-2,\ m_2=V^2\rho/\mu-2 \tag{25}$$

where A_j $(j=1,\dots 4)$ are the unknowns and will be determined based on the boundary conditions of the problems.

3 The Boundary Conditions and the Singular Integral Equation in the Continuous Contact Case

When the external load P is less than the critical value P_{cr}, the contact between the layer and the foundation will be continuous, and there will be no separation along the interface. Thus, the vertical displacement of the layer will be "0" at the interface. Also, the fact that the shear stress between the contacting components is "0" will result in frictionless contact. Therefore, the continuous contact problem should be solved under the following boundary conditions:

$$\sigma_y(x,h)=\left\{\begin{array}{cc}-p(x) & -a<x<a\\ 0 & x\le -a,\ \ x\ge a\end{array}\right\} \tag{26}$$

$$\tau_{xy}(x,h)=0\quad(-\infty\le x<\infty) \tag{27}$$

$$v(x,0)=0\quad(-\infty\le x<\infty) \tag{28}$$

$$\tau_{xy}(x,0)=0\quad(-\infty\le x<\infty) \tag{29}$$

where $p(x)$ is a priori unknown contact stress between the rigid punch and the layer on the contact area $(-a,a)$. Performing the boundary conditions given above, four of the unknown functions A_j can be obtained in terms of the unknown function $p(x)$ as follows:

$$A_j=\frac{1}{\mu}\int_{-a}^{a}p(t)A_j^pe^{I\alpha t}dt+\rho g\delta(\alpha)A_j^W\quad(j=1,\dots,4) \tag{30}$$

The unknown contact pressure $p(x)$ is determined based on the following condition:

$$\frac{\partial v(x,h)}{\partial x}=\frac{x}{R}\quad(-a<x<a) \tag{31}$$

Substituting the A_j into the mixed condition (31), the following singular integral equation can be obtained:

$$\begin{aligned}&\frac{1}{\pi}\int_{-a}^{a}p(t)\left[\frac{1}{t-x}+k_1(x,t)\right]dt\\&-\frac{1}{2\pi}\int_{-\infty}^{\infty}\frac{\mu}{\varphi_1}\left[\rho gW_1(\alpha)\delta(\alpha)\right]e^{-I\alpha x}d\alpha=\frac{\mu}{\varphi_1}\frac{x}{R}\end{aligned} \tag{32}$$

Note that the expressions related to the body forces vanish.

$$\frac{1}{2\pi}\int_{-\infty}^{\infty}\delta(\alpha)W_1(\alpha)e^{-I\alpha x}d\alpha=\lim_{\alpha\to 0}W_1(\alpha)=0 \tag{33}$$

Thus, the singular integral equation is reduced to the following structure:

$$\frac{1}{\pi}\int_{-a}^{a}p(t)\left[\frac{1}{t-x}+k_1(x,t)\right]dt=\frac{\mu}{\varphi_1}\frac{x}{R} \tag{34}$$

where

$$k_1(x,t)=\frac{1}{\varphi_1}\int_{0}^{\infty}(M_1(\alpha)-\varphi_1)\sin\alpha(t-x)d\alpha \tag{35}$$

The expressions for $M_1(\alpha)$, $W_1(\alpha)$, and φ_1 are given in Appendix A1.

To complete solution of the problem, contact stress $p(x)$ must satisfy the following equilibrium condition:

$$\int_{-a}^{a}p(t)dt=P \tag{36}$$

The integral Eq. (31) can be solved taking into account the equilibrium condition (36). However, the solution is only valid if the external load is less than P_{cr} $(0<P<P_{cr})$ which has not been determined yet. Thus, to determine the critical load P_{cr}, the contact stress between the layer and foundation $\sigma_y(x,0)$ should be evaluated. Substituting the A_j into (23), the contact stress on the interface is found as follows:

$$\sigma_y(x,0)=\frac{1}{\pi}\int_{-a}^{a}p(t)k_2(x,t)dt+\frac{1}{2\pi}\int_{-\infty}^{\infty}\delta(\alpha)\left[\rho gW_2(\alpha)\right]e^{-I\alpha x}d\alpha \tag{37}$$

Note that

$$\lim_{\alpha\to 0}\frac{1}{2\pi}\int_{-\infty}^{\infty}\delta(\alpha)W_2(\alpha)e^{-I\alpha x}d\alpha=-h \tag{38}$$

Thus, Eq. (37) becomes

$$\sigma_y(x,0)=\frac{1}{\pi}\int_{-a}^{a}p(t)k_2(x,t)dt-\rho gh \tag{39}$$

where

$$k_2(x,t)=\int_0^{\infty}M_2(\alpha)\cos\alpha(t-x)d\alpha \tag{40}$$

The expressions for $M_2(\alpha)$, $W_2(\alpha)$ are given in Appendix A2.

Introducing the following transformations

$$t=ar,\quad x=as \tag{41}$$

$$\alpha=z/h\quad \phi(r)=\frac{p(r)}{\mu} \tag{42}$$

the integral Eq. (34), the equilibrium condition (36), and the contact stress between the layer and foundation (39) may be expressed in the following forms:

$$\frac{1}{\pi}\int_{-1}^{1}\phi(r)\left[\frac{1}{r-s}+\frac{a}{h}k_1(s,r)\right]dr=\frac{1}{\varphi_1}\frac{a/h}{R/h}s\quad |r|\le 1 \tag{43}$$

$$\frac{a}{h}\int_{-1}^{1}\phi(r)dr=\frac{P}{\mu h} \tag{44}$$

$$\frac{\sigma_y(x,0)}{\mu}=\frac{1}{\pi}\int_{-1}^{1}\phi(r)\frac{a}{h}k_2(x,r)dr-\frac{\rho gh}{\mu} \tag{45}$$

Because the contact stress vanishes at the end points $x=-a$,$x=a$, the index of the integral Eq. (43) is -1 (Erdogan 1978). The solution of the integral equation can be expressed as

$$\varphi(r)=G(r)(1-r^2)^{1/2} \tag{46}$$

By using the Gauss–Chebyshev formulas (Erdogan 1978), the integral Eq. (43) can be converted to the system of algebraic equations as follows:

$$\sum_{i=1}^{N}W_i^N\left[\frac{1}{r_i-s_k}+\frac{a}{h}k_1(s_k,r_i)\right]G(r_i)=\frac{1}{\varphi_1}\frac{a/h}{R/h}s_k\quad k=1,\dots N+1 \tag{47}$$

where r_i and s_k are the roots of related Chebyshev polynomials and W_i^N is the weighting constant

$$r_i=\cos\left(\frac{i\pi}{N+1}\right)\quad i=1,\dots N \tag{48}$$

$$s_k=\cos\left(\frac{\pi}{2}\frac{2k-1}{N+1}\right)\quad k=1,\dots N+1 \tag{49}$$

$$W_i^N=\frac{1-r_i^2}{N+1} \tag{50}$$

Similarly, the equilibrium condition (44) and contact stress between the layer and foundation (45) become

$$\frac{a}{h}\pi\sum_{i=1}^{N}W_i^N g(r_i)=\frac{P}{\mu h} \tag{51}$$

$$\frac{\sigma_y(x,0)}{\mu}=\frac{a}{h}\sum_{i=1}^{N}W_i^N k_2(x,r_i)\,G(r_i)-\frac{\rho gh}{\mu} \tag{52}$$

It can be shown that the $N/2+1$ equation in (47) is automatically satisfied and results in the symmetry of the contact widths. Therefore, Eqs. (47) and (51) provide $N+1$ equations to determine the $N+1$ unknowns $G(r_i)$ and a/h. The system of equation is linear in terms of the $G(r_i)$ but highly nonlinear in terms of variable a/h. Therefore, considering the equilibrium condition (51), an iterative method is used to obtain unknowns. In addition, the solution must also ensure that the maximum contact stress between the layer and foundation (47) is equal to "0":

$$Max[\frac{\sigma_y(x,0)}{\mu}]=0 \tag{53}$$

Thus, to find the unknowns, $P_{cr}/(\mu h)$ and a/h are estimated at first. Then, $G(r_i)$ can be computed based on (47), and (51) and (53) are checked. The iteration keeps on until the "desired accuracy" obtained in (51) and (53) is reached. The value of $P/(\mu h)$ that satisfies Eq. (53) is the critical load $P_{cr}/(\mu h)$ and corresponding x/h is the location at which the interface separation begins (x_{cr}/h).

4 Boundary Conditions and the Singular Integral Equations in the Discontinuous Contact Case

Since the layer and foundation are not bonded to each other, the separation occurs for $P>P_{cr}$. The boundary conditions for the discontinuous moving contact problem can be written as follows:

$$\sigma_y(x,h)=\left\{\begin{array}{cc}-p(x) & -a<x<a\\ 0 & x\le -a,\ x\ge a\end{array}\right\} \tag{54}$$

$$\tau_{xy}(x,h)=0 \quad (-\infty\le x<\infty) \tag{55}$$

$$\frac{d}{dx}v(x,0)=f(x) \quad (b\le x<c,\ -c\le x<-b) \tag{56}$$

$$\tau_{xy}(x,0)=0 \quad (-\infty\le x<\infty) \tag{57}$$

where $f(x)$ is an unknown function that defines the separation between the layer and foundation on the separation region (b,c).

Taking the Fourier transforms of the boundary conditions (54–57), four of the unknown functions A_j can be obtained in terms of the unknown functions $p(x)$ and $f(x)$ as follows:

$$A_j=\frac{1}{\mu}\int_{-a}^{a}p(t)A_j^p e^{I\alpha t}dt+\int_{-\infty}^{\infty}f(x)A_j^m e^{I\alpha x}dx+\rho g\delta(\alpha)A_j^F \tag{56}$$

The unknown functions $p(x)$ and $f(x)$ will be determined by employing the following conditions:

$$\frac{\partial v(x,h)}{\partial x}=\frac{x}{R} \quad (-a<x<a) \tag{57}$$

$$\sigma_y(x,0)=0 \quad (b\le x<c,\ -c\le x<-b) \tag{58}$$

Substituting A_j into the conditions (57) and (58), the following singular integral equation system is obtained:

$$\frac{1}{\pi}\int_{-a}^{a}p(t_1)\left[\frac{1}{t_1-x_1}+k_{11}(x_1,t_1)\right]dt_1+\mu\frac{1}{\pi}\int_{b}^{c}f(t_2)\left[k_{12}(x_1,t_2)\right]dt_2$$
$$-\frac{\mu}{\beta_1}\frac{1}{2\pi}\int_{-\infty}^{\infty}\delta(\alpha)\left[\rho g W_{11}(\alpha)\right]e^{-I\alpha x_1}d\alpha=\frac{\mu}{\beta_1}\frac{x_1}{R} \tag{59}$$

$$\frac{1}{\pi}\int_{-a}^{a}p(t_1)\left[k_{21}(x_1,t_1)\right]dt_1+\mu\frac{1}{\pi}\int_{b}^{c}f(t_2)\left[\frac{\beta_2}{2}\left(\frac{1}{t_2+x_2}-\frac{1}{t_2-x_2}\right)+k_{22}(x_2,t_2)\right]dt_2$$
$$-\frac{1}{2\pi}\int_{-\infty}^{\infty}\delta(\alpha)\left[\rho g W_{12}(\alpha)\right]e^{-I\alpha x_2}d\alpha=0 \tag{60}$$

Note that

$$\lim_{\alpha\to 0}\frac{1}{2\pi}\int_{-\infty}^{\infty}\delta(\alpha)W_{11}(\alpha)e^{-I\alpha x}d\alpha=0 \tag{61}$$

$$\lim_{\alpha\to 0}\frac{1}{2\pi}\int_{-\infty}^{\infty}\delta(\alpha)W_{12}(\alpha)e^{-I\alpha x}d\alpha=-h \tag{62}$$

Hence, the singular integral equations become

$$\frac{1}{\pi}\int_{-a}^{a}p(t_1)\left[\frac{1}{t_1-x_1}+k_{11}(x_1,t_1)\right]dt_1$$
$$+\mu\frac{1}{\pi}\int_{b}^{c}f(t_2)\left[k_{12}(x_1,t_2)\right]dt_2=\frac{\mu}{\beta_1}\frac{x_1}{R} \tag{63}$$

$$\frac{1}{\pi}\int_{-a}^{a}p(t_1)\left[k_{21}(x_1,t_1)\right]dt_1+\mu\frac{1}{\pi}\int_{b}^{c}f(t_2)$$
$$\left[\frac{\beta_2}{2}\left(\frac{1}{t_2+x_2}-\frac{1}{t_2-x_2}\right)+k_{22}(x_2,t_2)\right]dt_2=\rho g h \tag{64}$$

where

$$k_{11}(x_1,t_1)=\frac{1}{\beta_1}\int_{0}^{\infty}(M_{11}(\alpha)-\beta_1)\sin\alpha(t_1-x_1)d\alpha \tag{65}$$

$$k_{12}(x_1,t_2)=\frac{1}{\beta_1}\int_{0}^{\infty}M_{12}(\alpha)\cos\alpha x_1\cos\alpha t_2 d\alpha \tag{66}$$

$$k_{21}(x_2,t_1)=\int_{0}^{\infty}M_{21}(\alpha)\cos\alpha(t_1-x_2)d\alpha \tag{67}$$

$$k_{22}(x_2,t_2)=\int_{0}^{\infty}M_{22}(\alpha)\sin\alpha x_2\cos\alpha t_2 d\alpha \tag{68}$$

The expressions for $M_{1i}(\alpha)$,$M_{2i}(\alpha)$, β_i are given in Appendix B.

For a complete solution of the problem, the following equilibrium and single-value conditions must be satisfied:

$$\int_{-a}^{a} p(t_1)dt_1 = P \tag{69}$$

$$\int_{b}^{c} f(t_2)dt_2 = 0 \tag{70}$$

For the numerical solution, the following normalizations are introduced:

$$t_1 = ar_1, \quad x_1 = as_1 \tag{71}$$

$$t_2 = \frac{c-b}{2}r_2 + \frac{c+b}{2}, \quad x_2 = \frac{c-b}{2}s_2 + \frac{c+b}{2} \tag{72}$$

$$\phi(r_1) = p(r_1)/\mu \tag{73}$$

Applying the normalizations, the integral equations become

$$\frac{1}{\pi}\int_{-1}^{1} \phi(r_1)\left[\frac{1}{r_1 - s_1} + \frac{a}{h}k_{11}(s_1, r_1)\right]dr_1 + \frac{1}{\pi}\int_{-1}^{1} f(r_2)\left[\frac{c-b}{2h}k_{12}(s_1, r_2)\right]dr_2 = \frac{1}{\beta_1}\frac{a/h}{R/h}s_1 \quad |r_i| \le 1 \tag{74}$$

$$\frac{1}{\pi}\int_{-1}^{1} \phi(r_1)\left[\frac{a}{h}k_{21}(s_1, r_1)\right]dr_1 + \frac{1}{\pi}\int_{b}^{c} f(r_2)\left[\frac{\beta_2}{2}\left(\frac{1}{r_2 + s_2 + 2\frac{c+b}{c-b}} - \frac{1}{r_2 - r_2}\right) + \frac{c-b}{2h}k_{22}(s_2, r_2)\right]dr_2 = \frac{\rho g h}{\mu} \tag{75}$$

Similarly, the equilibrium and single-value conditions become

$$\frac{a}{h}\int_{-1}^{1} \phi(r)dr = \frac{P}{\mu h} \tag{76}$$

$$\int_{-1}^{1} f(r_2)dr_2 = 0 \tag{77}$$

Because of the smooth contact, at the end points ($\mp a$,$\mp b$, and $\mp c$), the index of the integral Eqs. (74–75) is −1 (Erdogan 1978). The solution of the integral equations can be expressed as

$$\varphi(r_1) = G(r_1)(1 - r_1^2)^{1/2} \tag{78}$$

$$f(r_2) = H(r_2)(1 - r_2^2)^{1/2} \tag{79}$$

Applying the Gauss–Chebyshev integration formulas (Erdogan 1978), the integral Eqs. (74–75) can be reduced to the system of algebraic equations as follows:

$$\sum_{\xi=1}^{N} W_\xi^N\left[\frac{1}{r_\xi - s_k} + \frac{a}{h}k_{11}(s_k, r_\xi)\right]G(r_\xi) + \sum_{\xi=1}^{N} W_\xi^N\left[\frac{c-b}{2h}k_{12}(s_k, r_\xi)\right]H(r_\xi) = \frac{1}{\beta_1}\frac{a/h}{R/h}s_k \quad k = 1, \ldots N+1 \tag{80}$$

$$\sum_{\xi=1}^{N} W_\xi^N\left[\frac{a}{h}k_{21}(s_k, r_\xi)\right]G(r_\xi) + \sum_{\xi=1}^{N} W_\xi^N\left[\frac{\beta_2}{2}\left(\frac{1}{r_\xi + s_k + 2\frac{c+b}{c-b}} - \frac{1}{r_\xi - s_k}\right) + \frac{c-b}{2h}k_{22}(s_k, r_\xi)\right]H(r_\xi) = \frac{\rho g h}{\mu} \quad k = 1, \ldots N+1 \tag{81}$$

Similarly, the equilibrium (76) and single-value conditions (77) become

$$\frac{a}{h}\pi\sum_{\xi=1}^{N} W_\xi^N G(r_\xi) = \frac{P}{\mu h} \tag{82}$$

$$\sum_{\xi=1}^{N} W_\xi^N H(r_\xi) = 0 \tag{83}$$

Since the contact area under the punch is symmetrical, the $N/2+1$ equation in (80) is automatically satisfied. In (81), the additional equation (provided by $s_1, \ldots s_{N+1}$) is equivalent to the consistency conditions of the integral equation, and an equation corresponding to one of the s_k's will be used to determine a,b, and c with the equilibrium condition (82) and single-value condition (83). Thus, $2N+3$ unknowns, which are $G(r_\xi)$,$H(r_\xi)$, a, b, c, can be determined with $2N+3$ equations. The system of equations is linear in terms of $G(r_\xi)$ and $H(r_\xi)$ but highly nonlinear in terms of variables a,b, and c. Therefore, an iterative method should be used to obtain unknowns. In the iterative method, random initial values of a,b, and c are selected first. The system of Eqs. (80–81) is solved for $G(r_\xi)$ and $H(r_\xi)$ with these values. Then, Eqs. (82),

(83), and consistency condition are checked by substituting $G(r_i)$ and $H(r_i)$ into them. The iteration keeps on until the desired accuracy is obtained. The accuracy selected as 10^{-10} for the problem and iteration procedure is used based on the Newton–Raphson method.

Once $G(r_\xi)$,$H(r_\xi)$, a, b, c are determined, the displacement components $v(x, 0)$ can be obtained easily.

5 Numerical Results

In this part, numerical results for critical load, initial separation distance, separation regions, displacement on the interface, contact area under the punch, contact stress distributions under the punch and between the layer, and foundation are given for various dimensionless quantities such as moving velocity, body force, punch radius, and external load. Poisson's ratio is taken as $\nu = 0.25$(that is, $\kappa = 2$) in the following analysis. The values of μ and h should be considered fixed because they are related to more than one dimensionless quantity.

Note that if the sliding speed is chosen as $V = 0$, this problem is reduced to the static continuous and discontinuous contact problem of a layer (Çömez, 2019). Table 1 presents a comparison of the present study results and the results of Çömez (2019). It is seen that the present results are in line with the results of Çömez (2019).

Table 2 shows the variation of the critical load, initial separation distance, and contact area under the punch for various values of the moving velocity in the continuous contact case. Enhancing the moving velocity V causes the magnitude of the critical load to be small. In other words, the layer separates from the foundation readily when the punch moves faster. In addition, the contact area under the punch and the initial separation distance decrease with the increasing moving velocity. Table 3 shows the variation of the critical load, initial separation distance, and contact area under the punch for various values of the punch radius R. Increasing the punch radius (R) provides a wider contact area under the punch. As seen in Table 3, the magnitude of the critical load and initial separation distance does not change with the punch radius.

Table 1 Comparison of the contact area under the punch and separation regions with those from Çömez (2019) ($V^2\rho/\mu = 0,\ \rho gh/\mu = 1x10^{-6},\ R/h = 5,\ P/(\mu h) = 0.2 \times 10^{-3}$)

	a/h	b/h	c/h
This study	0.021856389	1.1084603	4.3090685
Çömez (2019)	0.021840995	1.1124342	4.3989408
Error (%)	0.070	0.358	2.085

Table 2 Variations of the contact width under the punch a/h, initial separation distance x_{cr}/h and critical load $P_{cr}/(\mu h)$ versus the moving velocity $V^2\rho/\mu$ ($\rho gh/\mu = 0.5 \times 10^{-6},\ R/h = 5,\ \kappa = 2$) (continuous contact)

$V^2\rho/\mu$	a/h	$P_{cr}/(\mu h)x10^6$	x_{cr}/h
0	0.007258628418	22.07035583	1.7700
0.2	0.006086206241	13.03324932	1.5240
0.4	0.004998004745	6.837585002	1.2620
0.6	0.003980143679	2.807589415	0.9720
0.8	0.003122026587	0.4107138716	0.5720

Figures 3, 4 and 5 delineate the contact stress distribution under the punch and between the layer and rigid foundation when the external load is less than the critical load. Note that contact stress between the layer and foundation equals the body force when the distance from the external load increases. From Fig. 3, it can be concluded that the contact stress under the punch decreases when the punch moves faster. An inverse relation can be observed in terms of the contact stress between the layer and foundation. Unlike other parameters, both the contact area and contact stress under the punch increase with the increase in the external load (Fig. 4). Note that the fact that the maximum value of the contact stress between the layer and foundation is zero for the critical load confirms the solution.

Figure 5 shows the variation of the contact stresses for various values of the punch radius R. When the punch radius increases, the external load is distributed over a larger area, and as a result, the peak value of the contact stress under the punch decreases. Another interesting result is that the contact stress between the layer and foundation does not change with the punch radius.

Table 4 shows the variation of the contact area under the punch and separation regions depending on the external load in the discontinuous contact case. When the external load increases, the punch penetrates the layer more,

Table 3 Variations of the contact width under the punch a/h, initial separation distance x_{cr}/h and critical load $P_{cr}/(\mu h)$ versus the punch radius R/h ($\rho gh/\mu = 0.5 \times 10^{-6},\ V^2\rho/\mu = 0.4,\ \kappa = 2$) (continuous contact)

R/h	a/h	$P_{cr}/(\mu h)x10^6$	x_{cr}/h
1	0.002235171709	6.837436382	1.2621
5	0.004998004745	6.837585002	1.2621
10	0.007068261792	6.837769903	1.2621
25	0.01117597847	6.838325729	1.2622
50	0.01580539832	6.839252247	1.2623

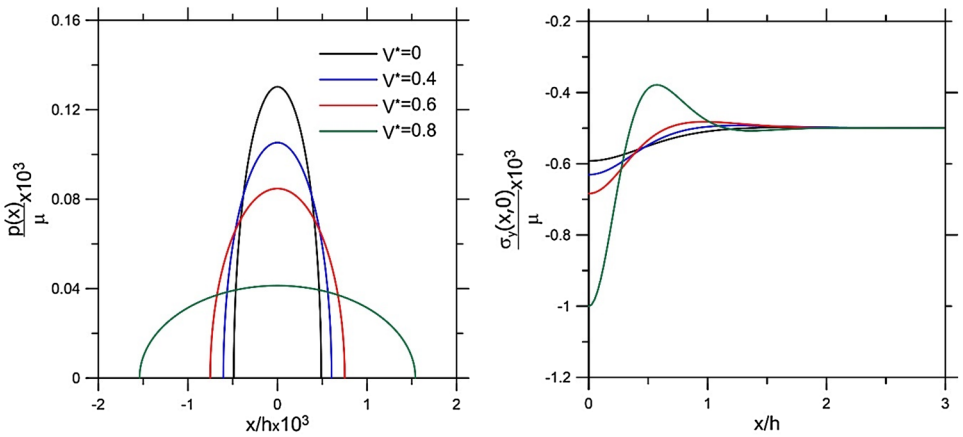

Fig. 3 Variations of the contact stress under the punch $p(x)/\mu$ and between the layer and substrate $\sigma_y(x,0)/\mu$ versus the moving velocity $V^* = V^2\rho/\mu$ $(P/(\mu h) = 0.1 \times 10^{-6},\ \rho gh/\mu = 0.5 \times 10^{-6},\ R/h = 5)$ (continuous contact)

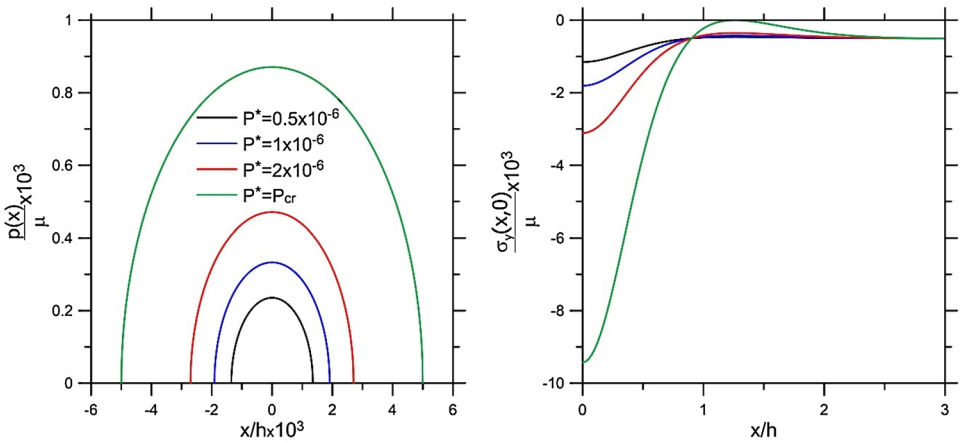

Fig. 4 Variations of the contact stress under the punch $p(x)/\mu$ and between the layer and substrate $\sigma_y(x,0)/\mu$ versus the external load $P^* = P/(\mu h)$ $(V^2\rho/\mu = 0.4,\ \rho gh/\mu = 0.5 \times 10^{-6},\ R/h = 5)$(continuous contact)

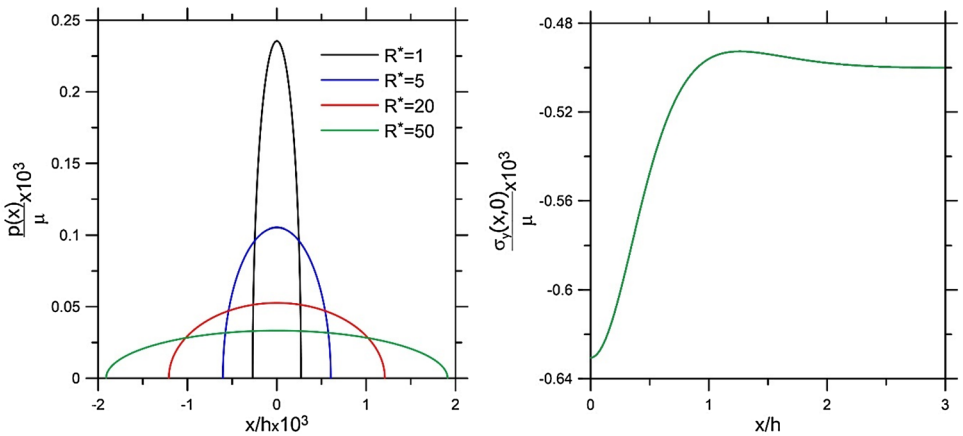

Fig. 5 Variations of the contact stress under the punch $p(x)/\mu$ and between the layer and substrate $\sigma_y(x,0)/\mu$ versus the punch radius $R^* = R/h$ $(V^2\rho/\mu = 0.4,\ P/(\mu h) = 0.1 \times 10^{-6},\ \rho gh/\mu = 0.5 \times 10^{-6})$ (continuous contact)

Table 4 Variation of the contact area under the punch and separation regions for various values of external load ($V^2\rho/\mu = 0.4$, $\rho gh/\mu = 0.5 \times 10^{-6}$, $R/h = 5$)(discontinuous contact)

$P/(\mu h)x10^6$	a/h	b/h	c/h
6.837585002	0.0049980034	1.2633748	1.263446
7.5	0.0052345015	1.0762518	1.5042101
10	0.0060442571	0.9101554	1.898055
12.5	0.0067576597	0.82346564	2.2433766

Table 5 Variation of the contact area under the punch and separation regions for various values of moving velocity ($P/(\mu h) = 30 \times 10^{-6}$, $\rho gh/\mu = 0.5 \times 10^{-6}$, $R/h = 5$)(discontinuous contact)

$V^2\rho/\mu$	a/h	b/h	c/h
0.000001	0.0084627113	1.397026	2.4013689
0.1	0.0088102641	1.1899883	2.6068677
0.2	0.0092336597	1.0036388	2.8619787

Table 6 Variation of the contact area under the punch and separation regions for various values of punch radius ($P/(\mu h) = 30 \times 10^{-6}$, $V^2\rho/\mu = 0.2$, $\rho gh/\mu = 0.5 \times 10^{-6}$)(discontinuous contact)

R/h	a/h	b/h	c/h
5	0.0092336597	1.0036388	2.8619787
10	0.013057995	1.0036945	2.8619392
20	0.018465743	1.0038256	2.8617904

and the contact area under the punch increases. The layer begins to separate from the layer easily with increasing external load values, and consequently, b/h decreases and c/h increases. Note that if the external load equals the critical load, the separation region closes (that is, $b/h = c/h$).

The variation of the contact area under the punch and separation regions with moving velocity is given in Table 5. When the punch moves faster, contact area under the punch increases and the separation starts more easily. Table 6 shows the variation of the contact area and separation region with punch radius. Note that the punch radius has not any influence on the separation region. However, the contact area under the punch increases with increasing values of the punch radius.

The variations of the contact stress between the punch and the layer $p(x)/\mu$, separation function $f(x)$, contact stress between the layer and foundation $\sigma_y(x,0)/\mu$, and the displacements on the interface $v(x,0)/h$ versus load $P^* = P/(\mu h)$ are shown in Fig. 6. Note that, unlike other parameters, both the peak values of the contact stress under the punch and the contact area increase with increasing values of the external load (Fig. 6a). The derivation of the vertical displacement $f(x)$ that defines the separation between the layer and foundation on the separation region (b, c) is not symmetrical (Fig. 6b). Thus, in the second integral equation, the $N/2+1$ equation should be considered as done in this study. The larger the value of external load, the longer the separation region (Fig. 6c). As expected, the vertical displacement $v(x,0)$ increases with the increasing values of the external load. Note that if the external load is equal to the critical load, the separation closes, and vertical displacement does not occur, as expected.

Figure 7 shows the variations of the contact stress between the punch and the layer $p(x)/\mu$, separation function $f(x)$, contact stress between the layer and foundation $\sigma_y(x,0)/\mu$, and the displacements on the interface $v(x,0)/h$ with the moving velocity $V^2\rho/\mu$. The peak values of the contact stress under the punch decrease when the punch moves faster (Fig. 7a). The separation region spreads with increasing values of moving velocity, and large displacement occurs at the interface (Fig. 7b–d). As the punch radius increases, the stress distributes over a wider area, and consequently, the peak values of the contact stress decrease (Fig. 8a). Note that the contact stress and vertical displacement at the interface do not change with the punch radius (Fig. 8b–d).

6 Conclusions

In this study, the dynamic continuous and discontinuous contact problems were discussed in the framework of the linear elasticity theory. The layer was indented by a rigid cylindrical punch, and body force was taken into account.

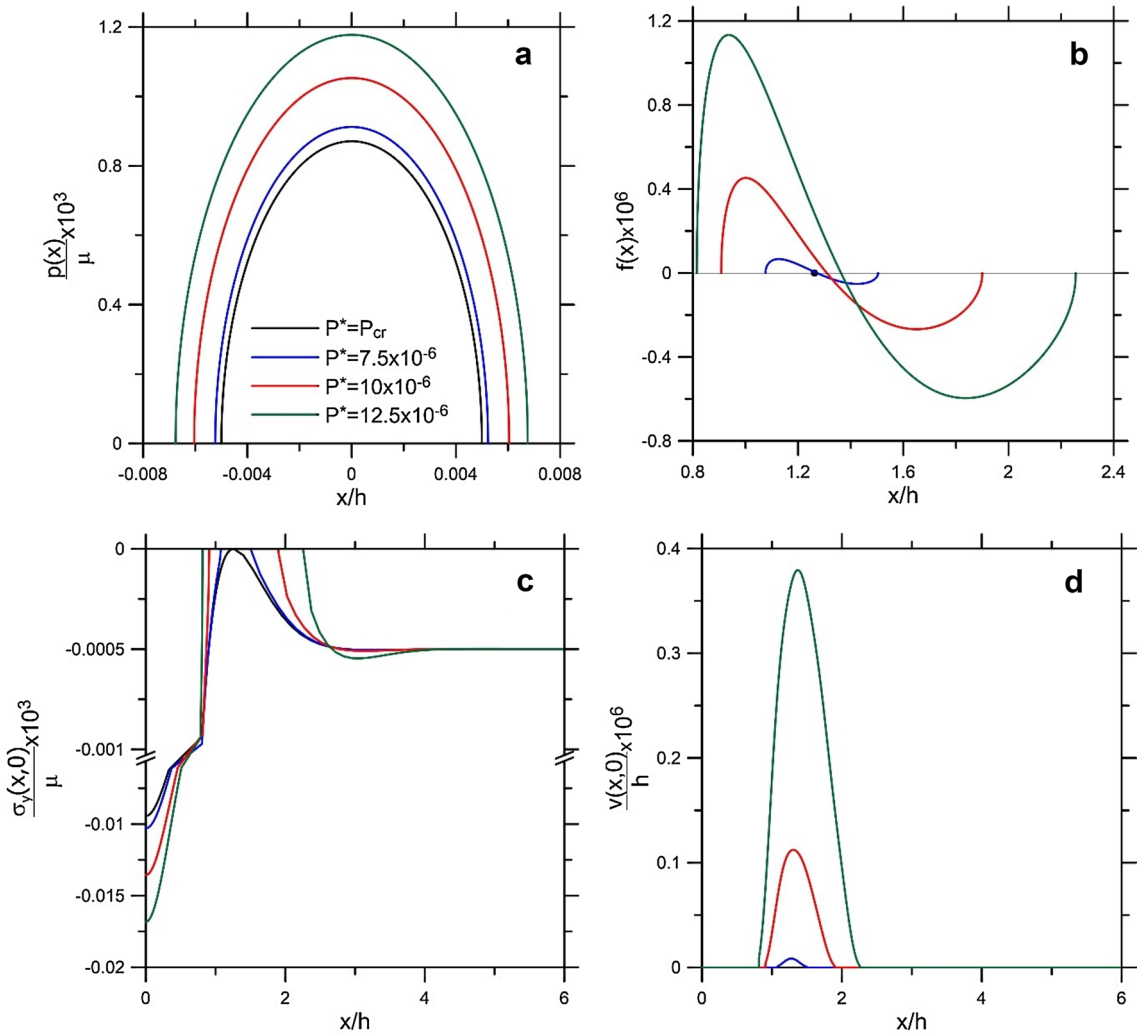

Fig. 6 Variations of the contact stress between the punch and the upper layer $p(x)/\mu$, $f(x)$, contact stress between the layer and substrate $\sigma_y(x,0)/\mu$, the displacements on the interface $v(x,0)/h$ versus load $P^* = P/(\mu h)$ with fixed parameters $V^2\rho/\mu = 0.4$, $\rho gh/\mu = 0.5 \times 10^{-6}$, $R/h = 5$. ($P_{cr} = 6.837585\text{x}10^{-6}$) (discontinuous contact)

General stress and displacement expressions for the moving continuous and discontinuous contact problems were obtained without using the superposition technique. Based on this study, the following conclusions can be outlined:

1. The critical load decreases when the moving velocity increases; that is, the layer easily separates from the foundation when the punch moves faster.
2. Both the contact area under the punch and the initial separation distance decrease when the punch moves faster.
3. The separation region and vertical displacement at the interface increase when the punch moves faster.
4. The punch radius does not influence the contact stress and vertical displacement at the interface.

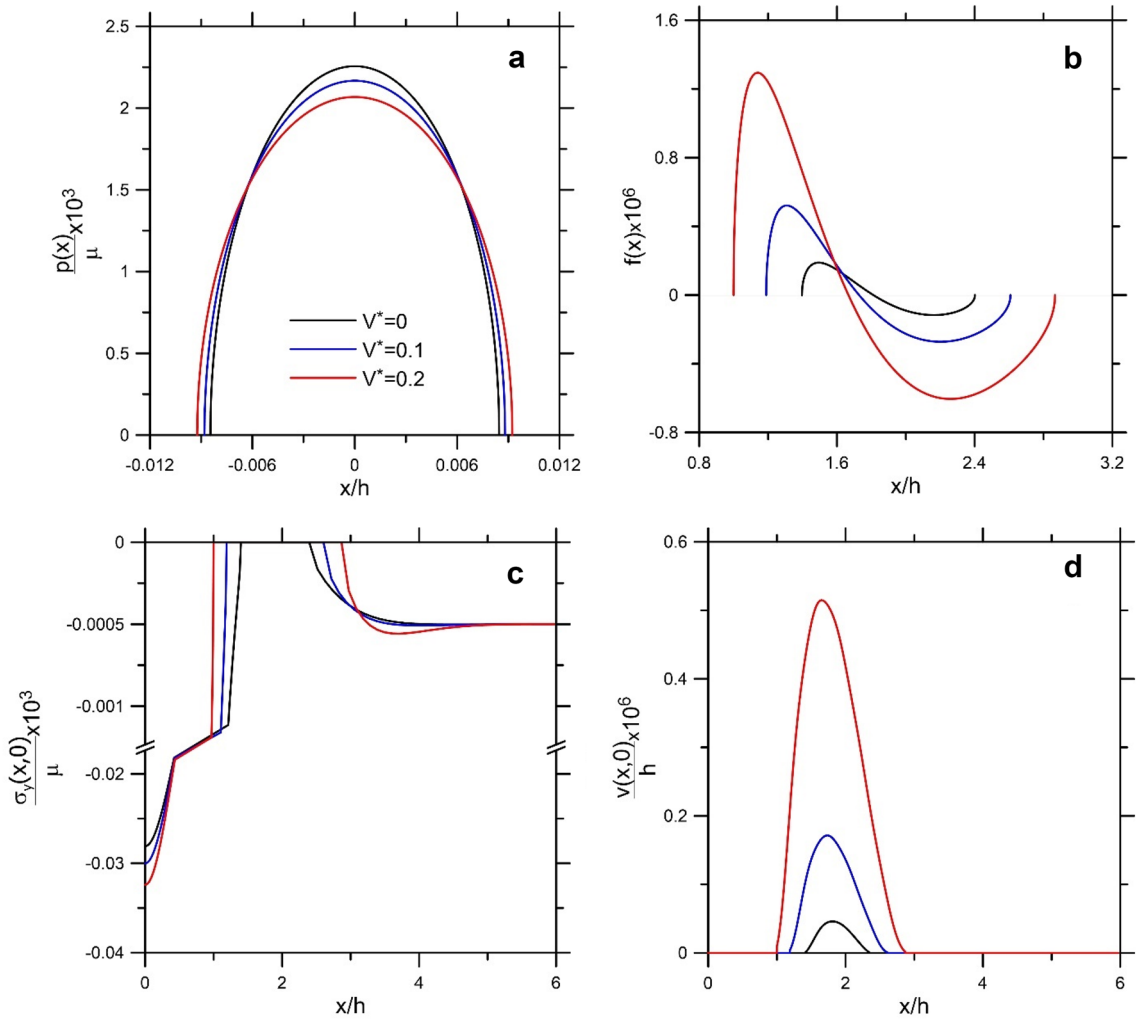

Fig. 7 Variations of the contact stress between the punch and the upper layer $p(x)/\mu$, $f(x)$, contact stress between the layer and substrate $\sigma_y(x,0)/\mu$, the displacements on the interface $v(x,0)/h$ versus moving velocity $V^* = V^2\rho/\mu$ with fixed parameters $P/(\mu h) = 30 \times 10^{-6}$, $\rho g h/\mu = 0.5 \times 10^{-6}$, $R/h = 5$ (discontinuous contact)

5. Unlike other parameters, both the peak values of the contact stress and the contact area between the punch and layer increase with increasing values of the external load.

Appendix

A1

The expressions of $M_1(\alpha)$, $W_1(\alpha)$, and φ_1 appearing in (26–29) and (32) are given as follows:

$$M_1(\alpha) = -\lim_{y\to 0}\ \alpha \sum_{j=1}^{4} A_j^p e^{n_j|\alpha|y} \tag{84}$$

$$W_1(\alpha) = -\lim_{y\to 0}\ \alpha\left(\alpha \sum_{j=1}^{4} A_j^F e^{n_j|\alpha|y} - \frac{\rho g/\mu}{\alpha^2(1-V^2\rho/\mu)}\delta(\alpha)\right) \tag{85}$$

$$\varphi_1 = \lim_{\alpha\to\infty}\ M_1(\alpha) \tag{86}$$

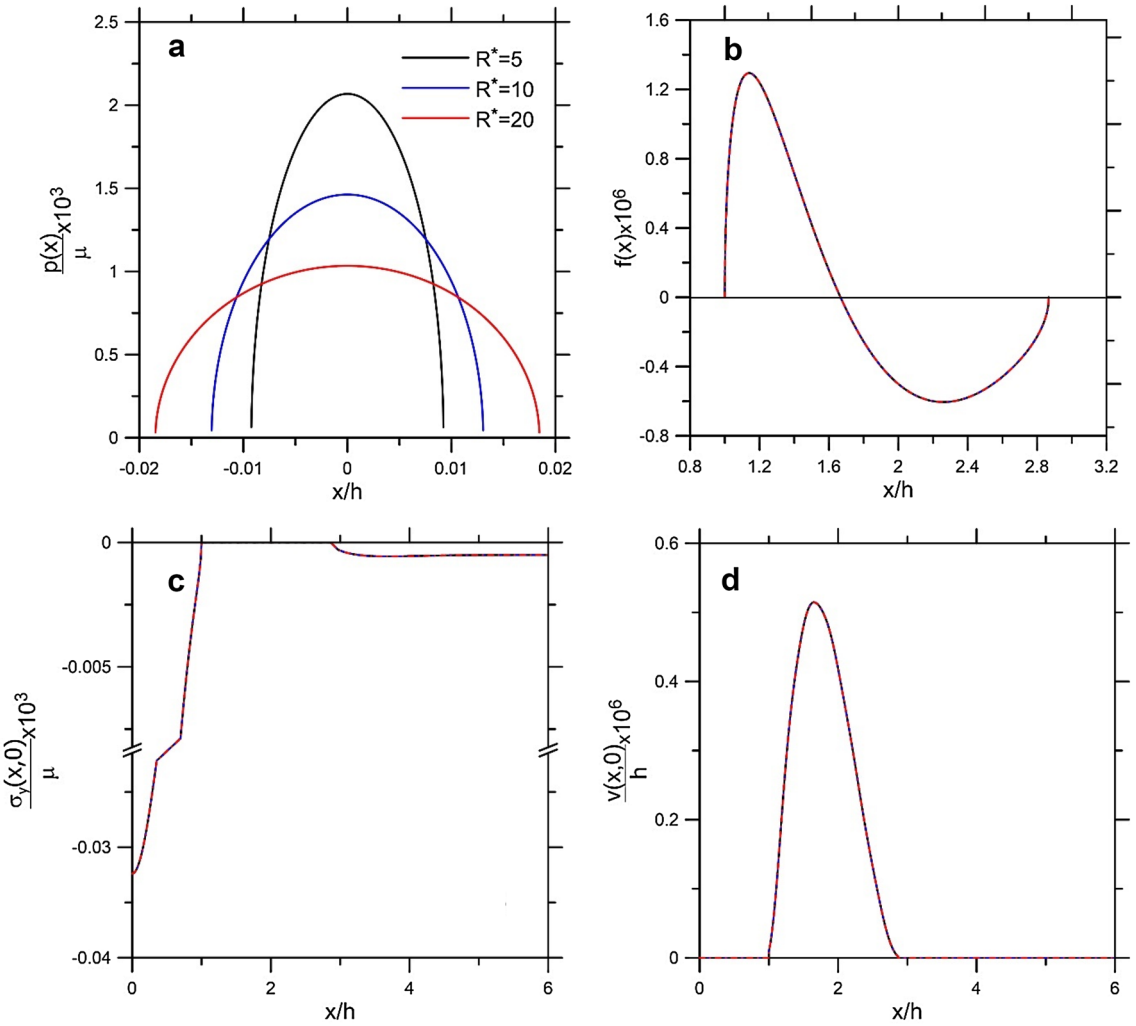

Fig. 8 Variations of the contact stress between the punch and the upper layer $p(x)/\mu$, $f(x)$, contact stress between the layer and substrate $\sigma_y(x,0)/\mu$, the displacements on the interface $v(x,0)/h$ versus punch radius $R^* = R/h$ with fixed parameters $P/(\mu h) = 30 \times 10^{-6}$, $V^2\rho/\mu = 0.2$, $\rho g h/\mu = 0.5 \times 10^{-6}$ (discontinuous contact)

A2

The expressions for $M_{21}(\alpha)$ and $W_{2i}(\alpha)$ appearing in (34) and (37) are given as follows:

$$M_2(\alpha) = \mathrm{Re}\left[\lim_{y\to 0} |\alpha|\left[2A_1^p n_1 e^{n_1|\alpha|y} - 2A_2^p n_2 e^{n_2|\alpha|y} - A_3^p \frac{1}{n_3} m_2 e^{n_3|\alpha|y} + A_4^p \frac{1}{n_4} m_2 e^{n_4|\alpha|y}\right]\right] \tag{87}$$

$$W_2(\alpha) = \mathrm{Re}\left[\lim_{y\to 0} |\alpha|\left[2A_1^F n_1 e^{n_1|\alpha|y} - 2A_2^F n_2 e^{n_2|\alpha|y} - A_3^F \frac{1}{n_3} m_2 e^{n_3|\alpha|y} + A_4^F \frac{1}{n_4} m_2 e^{n_4|\alpha|y}\right]\right] \tag{88}$$

Appendix B

The expressions of $M_{1i}(\alpha)$,$M_{2i}(\alpha)$, β_i $(i = 1, 2)$ appearing in (66–68) are given as follows:

$$M_{11}(\alpha) = \lim_{y\to 0} \alpha(A_1^p e^{n_1|\alpha|y} + A_2^p e^{n_2|\alpha|y} + A_3^p e^{n_3|\alpha|y} + A_4^p e^{n_4|\alpha|y}) \tag{89}$$

$$M_{12}(\alpha) = 2\mathrm{Re}[\lim_{y\to 0} \alpha(A_1^m e^{n_1|\alpha|y} + A_2^m e^{n_2|\alpha|y} + A_3^m e^{n_3|\alpha|y} + A_4^m e^{n_4|\alpha|y})] \tag{90}$$

$$M_{21}(\alpha) = \mu\mathrm{Re}\left[\lim_{y\to 0} |\alpha|(2A_1^p n_1 e^{n_1|\alpha|y} - 2A_2^p n_2 e^{n_2|\alpha|y} - A_3^p \frac{1}{n_3} m_2 e^{n_3|\alpha|y} + A_4^p \frac{1}{n_4} m_2 e^{n_4|\alpha|y})\right] \tag{91}$$

$$M_{21}(\alpha) = 2\mu \mathrm{Im}\left[\lim_{y\to 0} |\alpha|(2A_1^p n_1 e^{n_1|\alpha|y} - 2A_2^p n_2 e^{n_2|\alpha|y} - A_3^p \frac{1}{n_3} m_2 e^{n_3|\alpha|y} + A_4^p \frac{1}{n_4} m_2 e^{n_4|\alpha|y})\right] \quad (92)$$

$$\beta_1 = \lim_{\alpha\to\infty} M_{11}(\alpha) \quad (93)$$

$$\beta_2 = \lim_{\alpha\to\infty} M_{22}(\alpha) \quad (94)$$

References

Adibelli H, Comez I, Erdol R (2013) Receding contact problem for a coated layer and a half-plane loaded by a rigid cylindrical stamp. Arch Mech 65(3):219–236

Adıyaman G, Birinci A, Öner E, Yaylacı M (2016) A receding contact problem between a functionally graded layer and two homogeneous quarter planes. Acta Mech 227(6):1753–1766

Adıyaman G, Öner E, Birinci A (2017) Continuous and discontinuous contact problem of a functionally graded layer resting on a rigid foundation. Acta Mech 228(9):3003–3017

Çakıroğlu FL, Çakıroğlu M, Erdöl R (2001) Contact problems for two elastic layers resting on elastic half-plane. J Eng Mech 127(2):113–118

Chen P, Chen S (2012) Contact behaviors of a rigid punch and a homogeneous half-space coated with a graded layer. Acta Mech 223(3):563–577

Chen P, Peng J, Yu L, Yang Y (2017) The interfacial analysis of a film bonded to a finite thickness graded substrate. Int J Solids Struct 120:57–66

Chen P, Peng J, Liu H, Gao F, Guo W (2018) The electromechanical behavior of a piezoelectric actuator bonded to a graded substrate including an adhesive layer. Mech Mater 123:77–87

Chen P, Chen S, Peng J, Gao F, Liu H (2019) The interface behavior of a thin film bonded imperfectly to a finite thickness gradient substrate. Eng Fract Mech 217:106529.

Choi HJ (2009) On the plane contact problem of a functionally graded elastic layer loaded by a frictional sliding flat punch. J Mech Sci Technol 23(10):2703–2713

Civelek MB, Erdogan F (1975) The frictionless contact problem for an elastic layer under gravity. J Appl Mech 42(1):136–140

Comez I, Guler MA (2017) The contact problem of a rigid punch sliding over a functionally graded bilayer. Acta Mech 228(6):2237–2249

Comez I, Birinci A, Erdol R (2004) Double receding contact problem for a rigid stamp and two elastic layers. Euro J Mech A/Solids 23(2):301–309

Çömez İ (2010) Frictional contact problem for a rigid cylindrical stamp and an elastic layer resting on a half plane. Int J Solids Struct 47(7–8):1090–1097

Çömez İ (2019) Continuous and discontinuous contact problem of a functionally graded layer pressed by a rigid cylindrical punch. Euro J Mech A/Solids 73:437–448

Çömez İ, El-Borgi S, Kahya V, Erdöl R (2016) Receding contact problem for two-layer functionally graded media indented by a rigid punch. Acta Mech 227(9):2493–2504

El-Borgi S, Çömez I (2017) A receding frictional contact problem between a graded layer and a homogeneous substrate pressed by a rigid punch. Mech Mater 114:201–214

El-Borgi S, Abdelmoula R, Keer L (2006) A receding contact plane problem between a functionally graded layer and a homogeneous substrate. Int J Solids Struct 43(3–4):658–674

El-Borgi S, Usman S, Güler MA (2014) A frictional receding contact plane problem between a functionally graded layer and a homogeneous substrate. Int J Solids Struct 51(25–26):4462–4476

Erdogan F (1978) Mixed boundary value problems in mechanics. In: Nemat-Nasser S (ed) Mechanics today, vol 4. Pergamon Press.

Gecit MR (1980) A tensionless contact without friction between an elastic layer and an elastic foundation. Int J Solids Struct 16(5):387–396

Gecit MR, Erdogan F (1978) Frictionless contact problem for an elastic layer under axisymmetric loading. Int J Solids Struct 14(9):771–785

Guler MA, Erdogan F (2004) Contact mechanics of graded coatings. Int J Solids Struct 41(14):3865–3889

Guler MA, Erdogan F (2007) The frictional sliding contact problems of rigid parabolic and cylindrical stamps on graded coatings. Int J Mech Sci 49(2):161–182

Kahya V, Ozsahin TS, Birinci A, Erdol R (2007a) A receding contact problem for an anisotropic elastic medium consisting of a layer and a half plane. Int J Solids Struct 44(17):5695–5710

Kahya V, Birinci A, Erdol R (2007b) Frictionless contact problem between two orthotropic elastic layers. Int J Comput Math Sci 1:121–127

Kaya Y, Polat A, Özşahin TŞ (2020) Analytical and finite element solutions of continuous contact problem in functionally graded layer. Euro Phys J Plus 135(1):1–21

Ke LL, Wang YS (2006) Two-dimensional contact mechanics of functionally graded materials with arbitrary spatial variations of material properties. Int J Solids Struct 43(18–19):5779–5798

Ke LL, Wang YS (2007) Two-dimensional sliding frictional contact of functionally graded materials. Eur J Mech A/Solids 26(1):171–188

Liu TJ, Wang YS (2008) Axisymmetric frictionless contact problem of a functionally graded coating with exponentially varying modulus. Acta Mech 199(1–4):151–165

Liu TJ, Wang YS, Zhang C (2008) Axisymmetric frictionless contact of functionally graded materials. Arch Appl Mech 78(4):267–282

Liu TJ, Zhang C, Wang YS, Xing YM (2016) The axisymmetric stress analysis of double contact problem for functionally graded materials layer with arbitrary graded materials properties. Int J Solids Struct 96:229–239

Öner E, Adiyaman G, Birinci A (2017) Continuous contact problem of a functionally graded layer resting on an elastic half-plane. Arch Mech 69(1):53–73

Ozsahin TS, Taskıner O (2013) Contact problem for an elastic layer on an elastic half plane loaded by means of three rigid flat punches. Math Probl Eng 2013:1–14

Parel KS, Hills DA (2016) Frictional receding contact analysis of a layer on a half-plane subjected to semi-infinite surface pressure. Int J Mech Sci 108:137–143

Peng J, Wang Z, Chen P, Gao F, Chen Z, Yang Y (2019) Surface contact behavior of an arbitrarily oriented graded substrate with a spatially varying friction coefficient. Int J Mech Sci 151:410–423

Polat A, Kaya Y, Özşahin TŞ (2018) Analytical solution to continuous contact problem for a functionally graded layer loaded through two dissimilar rigid punches. Meccanica 53(14):3565–3577

Rhimi M, El-Borgi S, Said WB, Jemaa FB (2009) A receding contact axisymmetric problem between a functionally graded layer and a homogeneous substrate. Int J Solids Struct 46(20):3633–3642

Yan J, Li X (2015) Double receding contact plane problem between a functionally graded layer and an elastic layer. Euro J Mech A/Solids 53:143–150

Yan J, Mi C (2017a) Double contact analysis of multilayered elastic structures involving functionally graded materials. Arch Mech 69(3):199–221

Yan J, Mi C (2017b) On the receding contact between an inhomogeneously coated elastic layer and a homogeneous half-plane. Mech Mater 112:18–27

Yang J, Ke LL (2008) Two-dimensional contact problem for a coating–graded layer–substrate structure under a rigid cylindrical punch. Int J Mech Sci 50(6):985–994

Yilmaz KB, Comez I, Yildirim B, Güler MA, El-Borgi S (2018) Frictional receding contact problem for a graded bilayer system indented by a rigid punch. Int J Mech Sci 141:127–142